Co atoms on Bi$_2$Se$_3$ revealing a coverage dependent spin reorientation transition

New Journal of Physics

Co atoms on Bi_2Se_3 revealing a coverage dependent spin reorientation transition

T Eelbo[1,5]**, M Sikora**[2]**, G Bihlmayer**[3]**, M Dobrzański**[2]**,
A Kozłowski**[2]**, I Miotkowski**[4] **and R Wiesendanger**[1]

[1] Institute of Applied Physics, University of Hamburg, Jungiusstraße 11,
D-20355 Hamburg, Germany
[2] Faculty of Physics and Applied Computer Science, AGH University of
Science and Technology, 30 Mickiewicza Avenue, P-30-059 Krakow, Poland
[3] Peter Grünberg Institut and Institute for Advanced Simulation,
Forschungszentrum Jülich and JARA, D-52428 Jülich, Germany
[4] Department of Physics, Purdue University, 525 Northwestern Avenue,
West Lafayette, IN, USA
E-mail: teelbo@physnet.uni-hamburg.de

Abstract. We investigate Co nanostructures on Bi_2Se_3 by means of scanning tunneling microscopy and spectroscopy (STM/STS), x-ray absorption spectroscopy, x-ray magnetic dichroism (XMCD) and calculations using the density functional theory (DFT). In the single adatom regime we find two different adsorption sites by STM. Our calculations reveal these to be the fcc and hcp hollow sites of the substrate. STS shows a pronounced peak for only one species of the Co adatoms indicating different electronic properties of both types. These are explained on the basis of our DFT calculations by different hybridizations with the substrate. Using XMCD we find a coverage dependent spin reorientation transition from easy-plane toward out-of-plane. We suggest clustering to be the predominant cause for this observation.

[5] Author to whom any correspondence should be addressed.

With decreasing dimensionality and size of nanostructures, there is an increasing importance of the electronic interactions with the supporting substrate. This may lead to new electronic and magnetic properties, e.g. on substrates with a large spin–orbit interaction (SOI) giant magnetic anisotropies of isolated Co atoms were discovered [1] while on alkali metals these atoms behave as being quasi-free with vanishing magnetic anisotropy energies [2]. The interaction of nanostructures with the supporting substrate might also induce spin reorientation transitions (SRTs); for example, a monolayer of Fe on W(110) reveals an in-plane anisotropy while the anisotropy changes to out-of-plane if a second layer is grown on top [3]. The adsorption of individual magnetic adatoms and nanostructures on exotic surfaces, like three-dimensional topological insulators (TIs) is currently of high interest both from a fundamental point-of-view as well as in view of potential applications. TIs are a new class of materials characterized by a strong SOI which leads to gapless surface states with an odd number of Fermi-level crossings within the bulk band gap [4]. In the simplest case, a single Dirac cone consists of two spin-polarized linear dispersing branches and the crossing point, i.e. the Dirac point (DP), is protected by time reversal symmetry [5]. The time reversal symmetry is broken if magnetic impurities are introduced and the DP gets massive if species with a net out-of-plane magnetic moment are added [6–11]. For this reason, we investigated the properties of Co atoms after their adsorption on the surface of Bi_2Se_3. By means of scanning tunneling microscopy and spectroscopy (STM/STS), x-ray absorption spectroscopy (XAS) and x-ray magnetic circular dichroism (XMCD) we explore the electronic and magnetic properties of the transition metal (TM) adatoms. We explain our findings based on density functional theory (DFT) calculations performed in the generalized gradient approximation [12].

The experiments have been carried out in two separate ultrahigh vacuum systems. STM and STS experiments were performed at 5 K on Bi_2Se_3 single crystals *in situ* cleaved at low temperatures. Using electron beam evaporators Co was directly deposited onto the cold sample at 12 K to obtain well-isolated Co adatoms on the surface. To gain information about the local density of states (LDOS) electronic conductance (dI/dU) spectra were acquired by means of a lock-in technique using a modulation voltage $U_{mod} = 20$ mV and a frequency $f = 5$ kHz. The XAS and XMCD experiments have been carried out at the ID08 beamline at the European Synchrotron Radiation Facility. While the measurement temperature was about $T \approx 8$ K, the single crystals had to be cleaved at room temperature and immediately cooled down afterward. Co atoms have been deposited by using an electron beam evaporator with the substrate remaining in the measurement stage at a temperature of $T \approx 10$ K. X-ray absorption spectra were obtained in the total-electron-yield mode using almost 100% polarized light. Magnetic fields of up to 5 T were applied collinear to the incident beam. In addition, the sample was rotated from normal 0° to steep 70° incidence angle to obtain information about the in- and out-of-plane magnetic properties. All spectra have been normalized with respect to the incident beam intensity and the Co L_3 pre-edge intensity.

We used STM to address the local properties of the Co adatoms. Contrary to a recent work on Co monomers on Bi_2Se_3, where the authors concluded Co atoms to adsorb on Se top sites [13], we find two different types of Co atoms on Bi_2Se_3. Figure 1(a) proves that both species (in the following $Co_{A/B}$) occupy different adsorption sites which we illustrate by the white guidelines to the eyes. Regarding their apparent heights and shapes as well as the influence on the surrounding substrate further differences appear among both species. On the one hand, for the stabilization voltage chosen, Co_A shows a larger apparent height (≈ 0.7 Å) than Co_B (≈ 0.3 Å). On the other hand, in case of Co_A, the substrate shows an almost sixfold symmetric
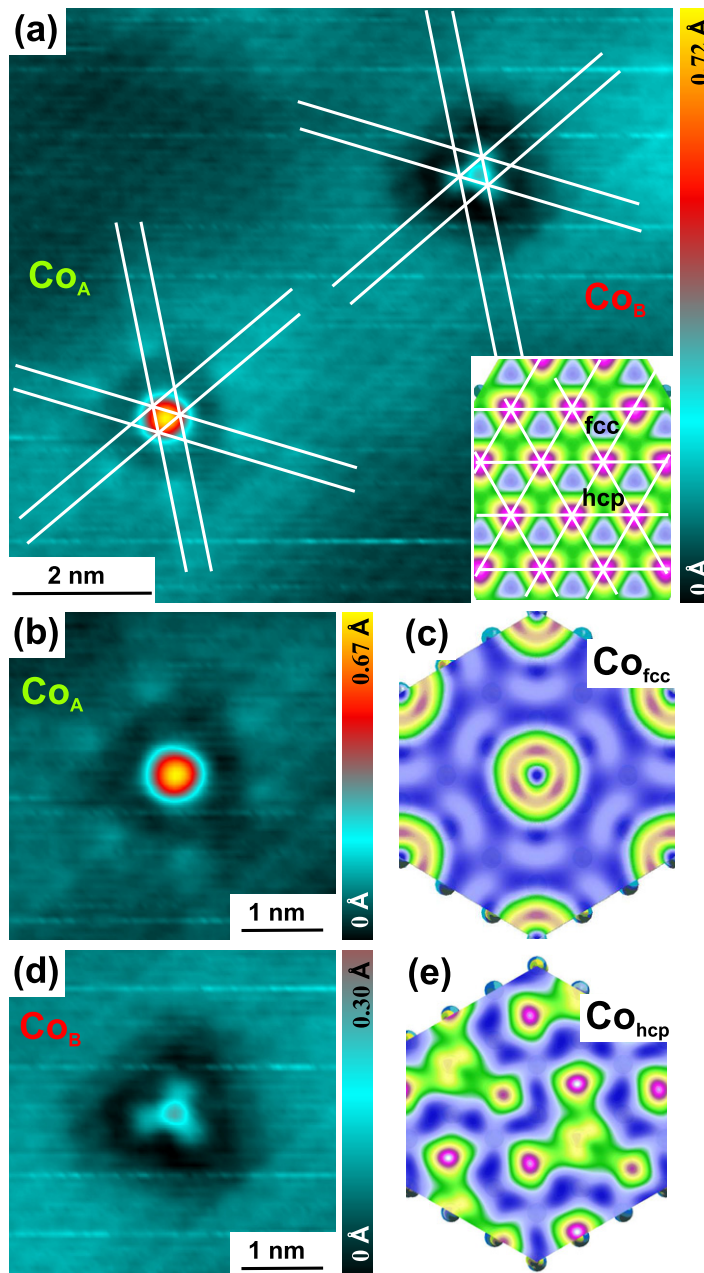
Figure 1. (a) STM topography of two different isolated Co adatoms on Bi_2Se_3. The tunneling parameters are $U = 0.2\,V$ and $I = 0.75\,nA$. The inset shows a theoretical simulation of the bare surface. The white lines are guide lines to the eyes representing Se top sites. (b), (d) Magnified views on both types of adsorbates showing the affected surface in their vicinity as well. (c), (e) Simulations of Co atoms adsorbed in the fcc and hcp hollow site for a bias voltage of $U = 0.1\,V$.

pattern in its vicinity whereas Co_B induces a threefold symmetric pattern, compare figures 1(b) and (d). Importantly, at no bias voltage, the Co adatoms appear as dark triangular depressions which generally would hint toward a substitution of Bi at its lattice site, which e.g. has been

found for Fe adatoms after room temperature annealing [14]. For a coverage of 0.01 monolayer equivalent (MLE) the relative abundance of both species is approximately three to one with a predominance of Co_A type adatoms indicating that the adsorption site of Co_A is energetically favorable. We note, that depending on the tunneling parameters (e.g. during STS) Co_B type atoms can be manipulated and afterward appear as Co_A. A change from Co_A toward Co_B has never been observed.

To elucidate our STM/STS observations, DFT calculations using the full-potential linearized augmented planewave method as implemented in the FLEUR-code[6] have been performed. The model comprises a $(\sqrt{3} \times \sqrt{3})R30°$ unit cell of four quintuple layers of Bi_2Se_3. We find the fcc hollow position to be the energetically most favorable adsorption site. Nevertheless, the hcp hollow position is unfavorable by only ≈ 90 meV per atom. For a comparison with the experimental data, STM topographies of the bare surface have been simulated using the vacuum density of states up to +100 mV, compare the inset of figure 1(a). At this voltage the Se atoms show up as bright triangles. Guidelines which cross at these positions reveal that $Co_{A/B}$ do occupy different hollow sites. Further simulations of Co atoms adsorbed in the fcc and hcp hollow sites reveal different appearances of both species, shown in figures 1(c) and (e). The good agreement between the simulated topographies and the experimental data let us conclude that Co_A is adsorbed in the fcc hollow site while Co_B is adsorbed in the hcp hollow site. This assignment is further supported by the relative abundance if the energy difference between both adsorption sites is taken into consideration.

In addition, the simulations indicate a relaxation of the Co atoms into the surface of Bi_2Se_3 in both cases by ≈ 0.2 Å. Opposite to theory, the experimentally resolved apparent heights differ significantly in case of fcc and hcp occupation. Thus, we relate the difference of the observed apparent heights to different hybridizations with the surrounding atoms resulting in different electronic properties for both species (adsorption sites). Therefore, the adatoms have been investigated by means of STS. Figure 2 shows STS spectra of pristine Bi_2Se_3 and Co/Bi_2Se_3. While for the pristine crystal the onset of the bulk valence (conduction) band is detected at ≈ -450 mV (≈ 0 mV), we find a global minimum (blue arrow) which we assign to the DP at -300 mV. The shift with respect to the Fermi level indicates that the crystal is naturally electron doped, being in agreement with previous observations [15, 16] and attributed to the existence of Se_{Bi} antisite defects [17]. Upon Co deposition of 0.01 MLE the off-dopant spectrum exhibits a global minimum (black arrow) at ≈ -350 mV, which hence depicts an additional shift of ≈ -50 mV of the DP with respect to the Fermi level. We conclude that Co further n-dopes the substrate and acts as a donor. In contrast to recent predictions [18, 19], no indication of a global surface band gap has been found after the deposition of Co adatoms. Regarding the STS spectra of the adatoms, no distinct resonances have been found in case of Co_A, whereas Co_B type adatoms reveal a pronounced peak at -400 mV. According to our theoretical calculations, the different electronic properties and the appearance of a resonance only in the hcp case are caused by different hybridizations of the Co 3d electrons with Bi_2Se_3, as is illustrated in figure 3. The fat band analysis of Co adatoms in the fcc (figure 3(a)) and hcp hollow site (figure 3(b)) reveal the DPs to be located at -0.55 and -0.25 eV, respectively. Spin up and spin down weights are defined with respect to the easy axes of both configurations, which are in-plane for fcc and out-of-plane for the hcp adsorption. While in case of hcp occupation the band structure shows two additional Co bands

---

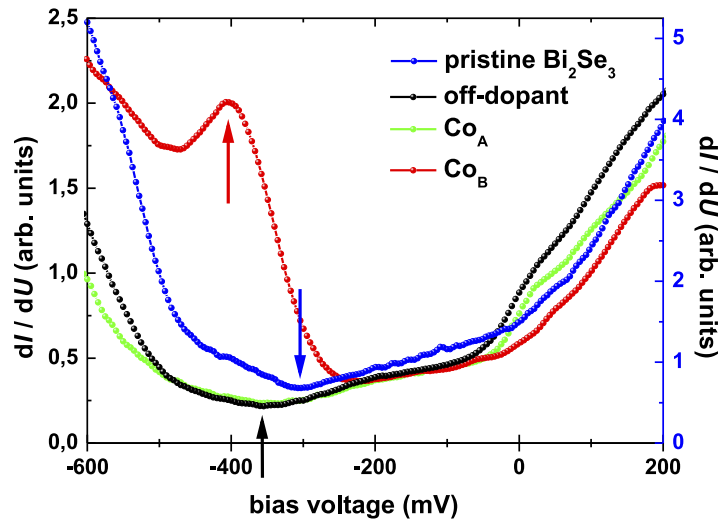[6] For a detailed description, see www.flapw.de.

Figure 2. STS of pristine Bi_2Se_3 (right y-axis) and 0.01 MLE Co/Bi_2Se_3 (left y-axis). The off-dopant spectrum has been acquired after Co deposition far away from any Co adatom. The blue and black arrows indicate the energetic position of the DP before and after Co deposition and, hence, reveal a shift of ≈ -50 mV. Tunneling parameters are $U = 0.2$ V and $I = 0.1$ nA.
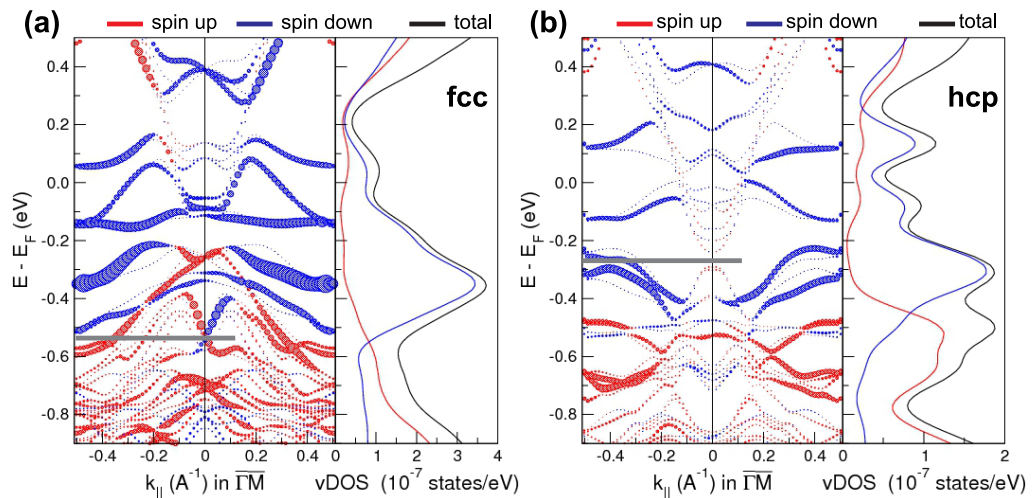

Figure 3. Fat band analysis and vacuum DOS of Co adsorbed in the fcc hollow site (a) and in the hcp hollow site (b). The red and blue lines indicate spin up and spin down states with respect to the easy axes while the black lines depict the total DOS. The size of the circles gives the spin-polarization of the states in a region above the surface. The gray lines depict the computed DPs at -0.55 and -0.25 eV for fcc and hcp occupation, respectively.

at ≈ -0.1 eV below the DP, these bands are shifted toward ≈ 0.3 eV above the DP in case of fcc. We also notice the different dispersion of these bands in the fcc and hcp geometry: while in the latter case the hybridization with the topmost valence band (mainly Bi p_z states [20]) leads to an

increase of the binding energy at the center of the Brillouin-zone, in the fcc-case the dispersion of the band is inverted. As a result, the Co-induced peak in the vacuum density of states (DOS) is energetically higher in the hcp than in the fcc case. Although the calculations were performed for a coverage of 0.33 MLE and, hence, the absolute positions of the peaks cannot be directly compared to the STS data, the differences between the fcc and hcp occupation are significant and can be related to the different STS observations, in particular the pronounced peak observed for Co_B.

The electronic and magnetic properties have been further tested by XAS and XMCD measurements, summarized in figure 4. A sketch of the experimental setup is depicted in figure 4(a). Different coverages ranging from 0.01 to 0.08 MLE have been investigated. Independent of the coverage, the shapes of the XAS spectra show no distinct multipeak structures besides a slight shoulder on the high-energy side of the Co L_3 edge at approximately 780.2 eV, compare figures 4(b) and (c). The XAS line shape suggests the Co atoms to be in the electronic configuration of $3d^7$ [21]. This result is in agreement to recent works on Fe/Bi_2Se_3 [22] as well as Fe and Co/Bi_2Te_3 [23] where the TM adatoms were found to be in their pristine configuration as well. Furthermore, the XAS spectra can be used to estimate the branching ratio (BR) which serves as an indicator of the spin character of the ground state of the adatoms[7] [24]. Within the coverage range investigated, we find a constant value of BR $= 0.84 \pm 0.01$ which suggests a high-spin ground state of the Co adsorbates. The inset in figure 4(b) shows the angular dependence of the XMCD signal normalized with respect to the L_3 XAS intensity, which can be used as an indicator for the easy axis of the Co adatoms. For the low coverage regime we find the signal strength for normal incidence angle to be enhanced by about 20% compared to the signal at grazing incidence angle. This suggests the easy axis to reside in the surface plane similar to Fe/Bi_2Se_3 [22] and contrary to predictions of an out-of-plane anisotropy for Co/Bi_2Se_3 in [13, 19]. The experimentally indicated easy-plane easy axis is particularly in line with our calculations, which predict an easy-plane magnetocrystalline anisotropy energy (MAE) in case of fcc hollow site occupation (Co_A; $K_{fcc} = -6$ meV) and an out-of-plane MAE in case of the hcp hollow site (Co_B; $K_{hcp} = +3$ meV), where K denotes the MAE per adatom. Taking the relative abundance into account (low coverage: $n_{Co_A}/n_{Co_B} = 3/1$) an easy-plane anisotropy is theoretically expected. The agreement further supports the assignment of the adsorption sites to the different types of Co adatoms. We note, that a site-dependent anisotropy has been reported before on metal substrates [25, 26] and as usual depends on the layer thickness, which—for our calculations—has been 0.33 MLE. Moreover, we investigated the anisotropy using the normalized L_3 XMCD intensity as a function of the coverage, see figure 4(d). Based on the accuracy level given for the estimation of the coverage, the relative L_3 XMCD/XAS intensities acquired at both angles suggest an in-plane easy axis at low coverages (0.01–0.04 MLE) and an out-of-plane easy axis for 0.08 MLE.

Unfortunately, the magnetic moments of the Co adatoms have not been saturated at the maximum magnetic field available 5 T and, thus, deducing the orbital and effective spin moments would be unreliable. However, the ratio (R) of orbital to effective spin moment[8] is independent of the saturation and can be used for conclusions about the investigated sample. In the regime of single atoms, we find $R = 0.33 \pm 0.02$, which is in good agreement

---

[7] BR: ratio of the integrated XAS of the L_3 edge divided by the sum of the integrated XAS of the L_3 and L_2 edges.
[8] R: ratio of orbital magnetic moment (m_L) to the sum of spin moment (m_S) and spin dipole moment (m_D) according to $R = m_L/(m_S + 7m_D)$, where the moments are given in μ_B/atom and are projected along the incident beam direction.
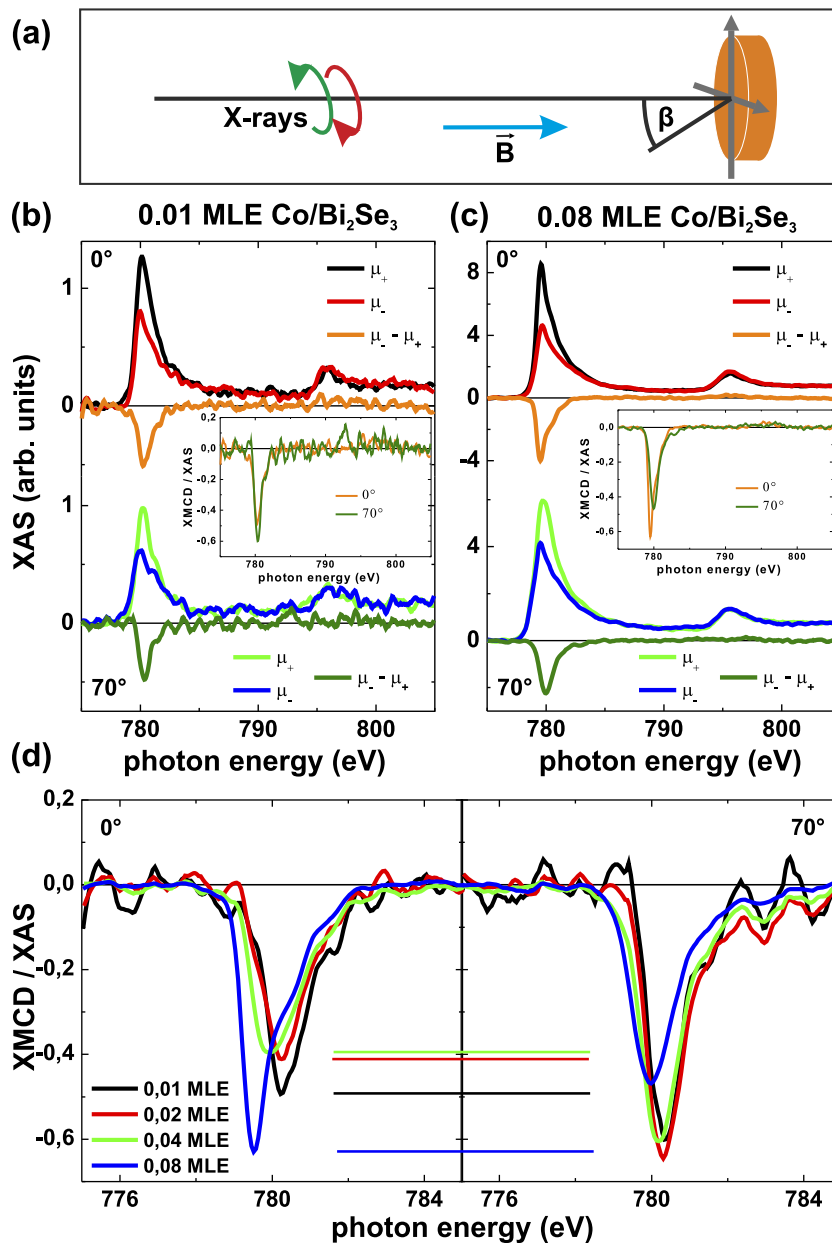
Figure 4. (a) Sketch of the experimental setup. The magnetic field can be applied parallel to the incident beam direction whereas the sample can be inclined with respect to this direction. (b) XAS and XMCD spectra for 0.01 MLE of Co/Bi_2Se_3 for normal (upper panel) and grazing (lower panel) incidence angle. The inset shows the XMCD signal strength normalized by the XAS L_3 peak height. (c) Spectra for an increased coverage of 0.08 MLE. (d) Normalized XMCD signals for a series of coverages ranging between (b) and (c) for normal (left panel) and grazing (right panel) incidence angle. The colored lines are guidelines to the eyes indicating differences between both angles.

with [13] and significantly larger than the Co bulk value [27]. The increase of the Co coverage toward 0.08 MLE goes hand in hand with a gain of the ratio until $R = 0.49 \pm 0.03$ which indicates relevant changes in the orbital and effective spin moments. Such a trend was observed before [13] although the orbital moment is expected to diminish upon increasing the mean cluster size [1]. This contradiction can be understood taking the SRT into consideration. In case of the low coverage (0.01 MLE) we find an easy-plane anisotropy, i.e. $m_L^x > m_L^z$ for z denoting the direction parallel to the surface normal. Hence, the ratio is given by $R^{0.01} = m_L^x/m_S^x = 0.33 \pm 0.02$. For the high coverage regime (0.08 MLE) we deduce an out-of-plane easy axis which, according to Bruno [28], means that $m_L^x < m_L^z$ in this case. Furthermore, in good agreement with our theoretical model, we can assume the magnetic spin moment to be independent of the orientation, i.e. $m_S^x \approx m_S^z$ ($1.17 \approx 1.15\,\mu_B$/atom). If the ratio of in-plane orbital moment and in-plane spin moment additionally remains constant while increasing the coverage, then an increase of the ratio given by $R^{0.08} = m_L^z/m_S^z = 0.49 \pm 0.03$ is possible and essentially driven by the SRT. We note, that these conclusions are based on the assumption of a vanishing spin dipole moment m_D and that the magnetic spin moments have been calculated for a coverage of 0.33 MLE.

In order to understand the SRT in more detail, we performed a series of STM/STS experiments at elevated coverages (up to 0.1 MLE) and determined the ratio of adatoms showing a resonance at $-400\,$mV, i.e. Co_B, to those not exhibiting this resonance. Although we observe slight changes of this ratio, no drastic modifications were found. Therefore, we experimentally rule out the possibility that a change of the relative population of fcc and hcp hollow sites upon increasing the total Co coverage might cause the observed SRT. Instead, we assign the transition to the decrease of the mean distance between the adatoms upon increasing the Co coverage. From this an emerging interaction as well as the growth of clusters seems plausible, which consequently causes serious modifications of the electronic properties as well as the anisotropy of the magnetic moments. This conclusion is supported by the XAS line shape showing a decrease of the high-energy shoulder at the Co L_3 edge upon increasing the coverage, compare figures 4(b) and (c). Furthermore, the series of coverage dependent XMCD spectra (figure 4(d)) shows that the peak position monotonically shifts downward in energy while increasing the coverage. The exact shape of the XAS spectra is determined by the average chemical state and the average crystal field of the ensemble probed by the x-ray beam, since the symmetry and the splitting of the crystal field as well as the chemical state might be slightly different for hcp and fcc occupation. Hence, we relate the variations of the XAS line shape and the shift of the L_3 peak position to changes of these quantities. The upcoming growth of clusters while the coverage is raised certainly influences both and, therefore, is a likely explanation for the mutation of the XAS/XMCD spectra. Note, that in the high coverage regime, similar to the low coverage regime, no gap opening has been detected for spectra acquired as far away from any impurity as possible, although the out-of-plane easy axis is evidenced by XMCD. A possible reason might be given in view of the clusters being the predominant cause of the variation of the anisotropy, since spectra in their vicinity have not been measurable because the tunneling conditions have not been sufficiently stable at these locations. In contrast, by the global technique of XMCD the clusters' influence can be easily detected. In general, our conclusions are supported by a recent study on bulk-doped Mn–Bi_2Se_3 where excess Mn clusters have been observed on the crystal's surface and suggested to significantly influence the surface magnetization of the sample [29].

In conclusion, by means of STM we find Co adatoms to occupy fcc and hcp hollow sites on Bi_2Se_3 after low temperature deposition. The irreversible switching from Co_B into Co_A as well as the employed DFT calculations let us assign the Co_A type adatoms to be adsorbed in fcc hollow sites. The DFT calculations further indicate different hybridization effects to be the cause for different electronic properties of both species found within the STS spectra. Using XMCD, we determine an easy axis of the magnetization in the surface plane for the low coverage regime, whereas it changes to out-of-plane upon increasing the Co coverage. Cluster formation is suspected to be responsible for the observed SRT.

Acknowledgments

References

[1] Gambardella P *et al* 2003 *Science* **300** 1130
[2] Gambardella P, Dhesi S S, Gardonio S, Grazioli C, Ohresser P and Carbone C 2002 *Phys. Rev. Lett.* **88** 047202
[3] Pietzsch O, Kubetzka A, Bode M and Wiesendanger R 2000 *Phys. Rev. Lett.* **84** 5212
[4] Fu L, Kane C L and Mele E J 2007 *Phys. Rev. Lett.* **98** 106803
[5] Kane C L and Mele E J 2005 *Phys. Rev. Lett.* **95** 226801
[6] Hor Y S *et al* 2010 *Phys. Rev.* B **81** 195203
[7] Chen Y L *et al* 2010 *Science* **329** 659
[8] Wray L A, Xu S Y, Xia Y, Hsieh D, Fedorov A V, Hor Y S, Cava R J, Bansil A, Lin H and Hasan M Z 2011 *Nature Phys.* **7** 32
[9] Okada Y *et al* 2011 *Phys. Rev. Lett.* **106** 206805
[10] Xu S-Y *et al* 2012 *Nature Phys.* **8** 616
[11] Chang C-Z *et al* 2013 *Science* **340** 167
[12] Perdew J P, Burke K and Ernzerhof M 1996 *Phys. Rev. Lett.* **77** 3865
[13] Ye M *et al* 2012 *Phys. Rev.* B **85** 205317
[14] Schlenk T *et al* 2013 *Phys. Rev. Lett.* **110** 126804
[15] Hor Y S, Richardella A, Roushan P, Xia Y, Checkelsky J G, Yazdani A, Hasan M Z, Ong N P and Cava R J 2009 *Phys. Rev.* B **79** 195208
[16] Bianchi M, Guan D, Bao S, Mi J, Brummerstedt Iversen B, King P D C and Hofmann P 2010 *Nature Commun.* **1** 128
[17] Urazhdin S, Bilc D, Tessmer S H, Mahanti S D, Kyratsi T and Kanatzidis M G 2002 *Phys. Rev.* B **66** 161306
[18] Liu Q, Liu C X, Xu C, Qi X L and Zhang S C 2009 *Phys. Rev. Lett.* **102** 156603
[19] Schmidt T M, Miwa R H and Fazzio A 2011 *Phys. Rev.* B **84** 245418
[20] Zhang H, Liu C X, Qi X L, Dai X, Fang Z and Zhang S C 2009 *Nature Phys.* **5** 438
[21] van der Laan G and Kirkman I W 1992 *J. Phys.: Condens. Matter* **4** 4189
[22] Honolka J *et al* 2012 *Phys. Rev. Lett.* **108** 256811
[23] Shelford L R, Hesjedal T, Collins-McIntyre L, Dhesi S S, Maccherozzi F and van der Laan G 2012 *Phys. Rev.* B **86** 081304
[24] Thole B T and van der Laan G 1988 *Phys. Rev.* B **38** 3158
[25] Błoński P, Lehnert A, Dennler S, Rusponi S, Etzkorn M, Moulas G, Bencok P, Gambardella P, Brune H and Hafner J 2010 *Phys. Rev.* B **81** 104426

[26] Khajetoorians A A, Schlenk T, Schweflinghaus B, dos Santos, Dias M, Steinbrecher M, Bouhassoune M, Lounis S, Wiebe J and Wiesendanger R 2013 *Phys. Rev. Lett.* **111** 157204

[27] Chen C T, Idzerda Y U, Lin H J, Smith N V, Meigs G, Chaban E, Ho G H, Pellegrin E and Sette F 1995 *Phys. Rev. Lett.* **75** 152

[28] Bruno P 1989 *Phys. Rev.* B **39** 865

[29] Zhang D *et al* 2012 *Phys. Rev.* B **86** 205127